Available online at www.sciencedirect.com
SCIENCE DIRECT
Catalysis Today 99 (2005) 137–142
CATALYSIS TODAY
www.elsevier.com/locate/cattod

Synthesis of catalytic materials on multiple length scales: from mesoporous to macroporous bulk mixed metal oxides for selective oxidation of hydrocarbons

Moises A. Carreon, Vadim V. Guliants*

Department of Chemical and Materials Engineering, University of Cincinnati, Cincinnati, OH 45221-0012, USA

Available online 28 December 2004

Abstract

A short review is provided of the principles guiding the synthesis of mesoporous and macroporous *bulk mixed metal oxides* on multiple length scales in the presence of surfactant mesophases and colloidal arrays of monodisperse spheres, respectively. Emerging catalytic applications of these novel bulk metal oxide phases in selective oxidation of hydrocarbons are described and discussed.

Keywords: Molecular design; Mixed metal oxides; Mesoporous oxides; Macroporous oxides; Selective oxidation

1. Introduction

The bulk mixed metal oxides have shown in recent decades considerable promise for the selective oxidation and ammoxidation of lower alkanes [1–7]. Vanadium-phosphorus-oxide, the industrial catalyst for the oxidation of *n*-butane to maleic anhydride, is among the most notable examples of bulk mixed metal oxide catalysts, which also shows significant selectivity in pentane oxidation to phthalic and maleic anhydrides and propane ammoxidation to acrylonitrile, as demonstrated by Trifirò and coworkers [8–12]. Keggin-type heteropoly-compounds are promising for the oxidation of propane and isobutane, whose composition can be tuned to direct the reaction either to the formation of olefins or oxygenated compounds [3]. The recently reported bulk mixed Mo–V–Sb–Nb oxides [13,14] are active and selective in propane oxidation to acrylic acid. These and other efficient catalysts for propane ammoxidation are based on the bulk mixed metal oxides, such as promoted vanadium antimonates with the rutile structure [15] and Mitsubishi-type multicomponent vanadium molybdates possessing the orthorhombic structure [16].

The rational assembly of complicated mixed metal oxide phases from atoms and molecules to nano- and macroscale entities remains one of the most difficult challenges of today's catalytic materials science. The ability to control the mixed metal oxide assembly on multiple length scales, from a few angstroms to microns, will result in unique porous structures with finely tuned surface active sites that are particularly desirable for applications in heterogeneous catalysis. Meso- and macroscale self-assembly approaches represent particularly promising routes to design novel catalytic phases with unique pore structures, flexible compositions and tunable surface active sites. The proposed self-assembly pathways for mesostructured bulk metal oxides are illustrated in Fig. 1. For example, the formation of highly ordered mesostructures containing cylindrical mesopores may take place via charge matching interactions between the inorganic species at the interface with a pre-existing hexagonal lyotropic liquid crystal phase. The template removal leads to highly ordered structures exhibiting ~2–33 nm mesopores [17–19].

The macroscale templating approach consists of three distinct processing steps shown in Fig. 2. First, the interstitial voids of the monodisperse colloidal latex sphere (~100 nm to 50 μm in diameter) arrays are filled with precursors of various classes of materials, such as ceramics, semiconductors,

* Corresponding author.
E-mail address: vadim.guliants@uc.edu (V.V. Guliants).

0920-5861/$ – see front matter © 2004 Elsevier B.V. All rights reserved.
doi:10.1016/j.cattod.2004.09.033

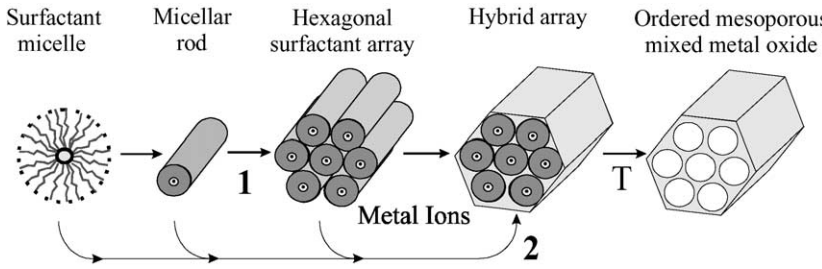

Fig. 1. Formation of 2D hexagonal *mesoporous* structures in the presence of surfactant mesophases.

metals, monomers, etc. In the second step, the precursors condense around the spheres and form a solid framework. Finally, the spheres are removed by either calcination or solvent extraction leading to the formation of 3D ordered macroporous structures [20]. In this paper, we briefly discuss recent advances in multiscale self-assembly of *bulk* mixed metal oxides in our laboratory and around the world as well as emerging catalytic applications of these novel phases in selective alkane oxidation reactions. Therefore, the topics of ordered mesoporous *silica* containing surface metal oxide components as well as meso- and macroporous *catalytic supports* are outside the scope of this review.

2. Surfactant-assisted self-assembly of mesostructured mixed metal oxides

Two mechanistic pathways were proposed by Mobil researchers [17–19] to explain the formation of mesostructured metal oxides: (1) condensation and cross-linking of the inorganic species at the interface with a pre-existing hexagonal lyotropic liquid crystal (LC) phase; (2) ordering of the surfactant molecules into the 2D hexagonal mesophase mediated by the inorganic species and followed by their condensation and cross-linking (Fig. 1). In both pathways, the inorganic species, which are negatively charged at the high synthesis pH preferentially interact with the positively charged alkylammonium head groups of the surfactant molecules and condense into a solid, continuous framework. The resulting organic–inorganic mesostructure could be alternatively viewed as a hexagonal array of surfactant micellar rods embedded in the inorganic matrix. The surfactant removal produces an open ordered mesoporous hexagonal framework. These mesophases with pore diameters > 2.5 nm generally display type IV nitrogen adsorption–desorption isotherms at 77 K characteristic of mesoporous materials with ordered unimodal pore size distribution. The initial work of the Mobil researchers involved only alkaline-catalyzed preparations and materials reported in these papers are referred to as MCM-41 (*P6mm* 2D hexagonal phase), MCM-48 (*Ia3d* cubic phase) and MCM-50 (lamellar phase). Many other ordered pore structures corresponding to different surfactant assemblies have been synthesized [21–23]. Several aspects of these ordered mesoporous transition metal oxide (TMS) family have been reviewed by Antonelli and Ying [24].

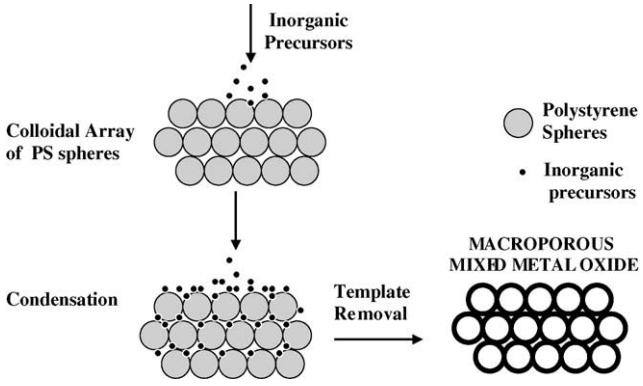

Fig. 2. General procedure for the synthesis of highly ordered *macroporous* mixed metal oxide phases.

The synthesis of bulk mixed metal oxides in the presence of surfactant mesophases offers the possibility to design novel catalytic phases with high surface areas, controlled porosities, tunable surface compositions and improved catalytic performance. One of the most interesting mixed metal oxides is the vanadium-phosphorus-oxide (VPO) catalyst for *n*-butane oxidation to maleic anhydride, which is the only industrial process of vapor-phase oxidation of an alkane [8–12,25]. Several reports exist on the synthesis of mesostructured VPO phases. Iwamoto and coworkers [26] reported the synthesis of mesostructured hexagonal vanadium-phosphorus-oxides using alkyltrimethyl ammonium surfactants (C_{12}–C_{16}). However, the mesostructure in these materials was lost upon calcination. Doi and Miyake [27] reported the synthesis of a novel hexagonal mesostructured VPO compound from the VPO precursor, $VOHPO_4{\cdot}0.5H_2O$, by surfactant intercalation and subsequent hydrothermal treatment. However, these materials suffered from poor thermal stability and low phosphorus content that are detrimental for their use as heterogeneous catalysts. Amoros and coworkers [28] described the synthesis of hexagonal mesostructured oxovanadium phosphates, denoted as ICMUV-2. However, the surfactant removal from their vanadium phosphates resulted in the collapse of the mesostructure. Mizuno et al. [29] described the synthesis of hexagonal, cubic and lamellar mesostructured vanadium-

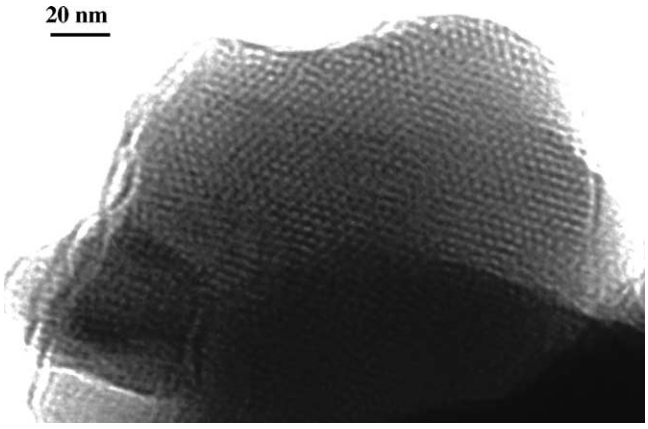

Fig. 3. TEM image of as-synthesized *mesostructured* hexagonal VPO phase along the *c*-axis [54].

phosphorus-oxides that lost structural order upon calcination. We recently reported novel hexagonal, cubic and lamellar VPO phases, which displayed improved thermal stability, desirable chemistries (i.e. the P/V ratios and vanadium oxidation states), and pore structures for the partial oxidation of lower alkanes [30–32]. Fig. 3 shows the TEM image of mesostructured VPO displaying a 2D hexagonal array of cylindrical ~30 Å pores. It was demonstrated in these studies that the V oxidation state and the surface P/V ratios could be tuned, respectively, via post-synthesis thermal treatment (i.e., oxidizing versus reducing atmosphere) and inorganic–organic interfacial chemistry (i.e., the surfactant functionality) [30,33]. The N_2 adsorption–desorption isotherm measurements indicated that these novel VPO phases had a broad size distribution in the micropore range. However, the complete surfactant removal and achievement of thermal stability for the mesoporous VPO system still represents a major challenge [33]. The incomplete cross-linking of the VPO framework, its redox properties and the low Tammann temperature of the constituent oxides have so far prevented the preparation of thermally stable mesoporous VPO phases.

Other mesostructured mixed metal oxides promising for selective oxidation catalysis that has been successfully prepared include: Nb/Ta, V–Nb and Mg–V oxides. Mesoporous mixed Nb/Ta ~ 1 oxide displaying a wormhole pore structure were prepared via neutral templating method by employing a nonionic surfactant, Pluronic P-123, as the structure directing agent [34]. Interestingly, the resultant mesostructure displayed not only improved thermal stability, but also the presence of nanocrystalline walls. However, as the crystallinity of the mesostructure increased with calcination time, the BET surface areas decreased from 168 to 22 m^2/g suggesting the densification of the final mesostructure. In order to prevent the surface area decrease, Antonelli et al. [35] employed the ligand-assisted method to prepare mesoporous V–Nb oxides (5–15 mol% V in mesoporous niobium oxide). Primary alkyl amines were used as structure directing agents. Although high surface area composites (500–830 m^2/g) were reported, only disordered wormhole pore structures were obtained, which exhibited ~2.0–2.3 nm thick walls. Chao and Ruckenstein succeeded in the preparation of mesoporous Mg–V oxides (Mg/V = 0.5–10) by employing cetyltrimethyl ammonium bromide and hexadecylamine as templates [36,37]. These novel mesostructures exhibiting relatively high surface areas (i.e. 70–250 m^2/g) and wormhole-like pores are promising for oxidative dehydrogenation of alkanes. The pore size of these composites was fine-tuned as a function of the synthesis pH. They proposed a self-assembly mechanism in which anionic polyvanadate species associated with a Mg^{2+} cation condenses around positively charged surfactant micelles. The improved thermal stability of this system was attributed to the incorporation of Mg cations into the inorganic oxovanadium framework.

Most of the reported mesostructured transition mixed metal oxides display limited thermal stability. High thermal stability of mesoporous phases is perhaps the most critical requirement for their applications in heterogeneous catalysis. In general, thermal stability of mesostructured metal oxide phases depends on (1) the degree of charge-matching at the organic–inorganic interface, (2) the strength of interactions between inorganic species and surfactant headgroups, (3) the flexibility of the M–O–M bond angles in constituent metal oxides, (4) the Tammann temperature of the metal oxide and (5) the occurrence of redox reactions in the metal oxide wall.

The *charge-matching* at the organic–inorganic interface enables control over the wall composition and facilitates cross-linking of the inorganic species into a robust mesostructured network. The knowledge of the electrokinetic behavior (i.e. the isoelectric points) of the inorganic species in solution is required for fine-tuning electrostatic and other interactions at the inorganic–organic interface in order to obtain thermally stable mesoporous phases [38]. The presence of strong *covalent bonds* between metal oxide species and surfactant headgroups, e.g. metal-N, requires harsh conditions for surfactant removal, such as combustion, which may lead to mesostructure collapse. Similarly, rigid M–O–M bond angles that are unable to accommodate the curvature of the inorganic–organic interface may result in the formation of only lamellar or dense metal oxide phases. On the other hand, metal oxide species should possess low lattice mobility at elevated temperatures in order to prevent transformation of mesostructured metal oxides into more thermodynamically stable dense phases. The mobility of metal ions or atoms in a crystalline metal oxide increases rapidly in the vicinity of its *Tammann temperature* defined as $0.5–0.52T_m$, where T_m is the melting point in K [39]. Therefore, it is not surprising that the low Tammann temperature of some transition metal oxides (V_2O_5, 472 K; MoO_3, 534K; Nb_2O_5, 892 K) [40,41] translated into limited thermal stability of the corresponding mesostructures. Finally, the structural collapse of mesophases may be caused by *redox reactions* occurring in the metal oxide wall during surfactant removal or catalytic reaction. The existing

strategies together with emerging new synthesis routes to improve the thermal stability of mesoporous metal oxides are expected to lead to the development of novel mesoporous catalysts with unique catalytic properties. Furthermore, they represent model catalytic systems that will enable improved fundamental understanding of the relationships between the molecular structure and catalytic properties of a broad range of industrially relevant catalytic systems.

3. Colloidal sphere templating of macroporous mixed metal oxides

Macroscale-templated synthesis of bulk nanocrystalline mixed metal oxides is an attractive approach for the design of catalytic phases that possess remarkable ordering on the macroscale (>50 nm for pore architectures). In particular, templating against opaline arrays of colloidal spheres (~100 nm to 50 μm in diameter) offers a general route to macroporous materials displaying controlled pore sizes, high surface areas (>100 m^2/g), and highly ordered three-dimensional porous structures, which are very attractive for catalytic applications. The success of forming macroporous ordered structures is mainly determined by van der Waals interactions, wetting of the template surface, filling of the voids between the spheres and volume shrinkage of the precursors during solidification process [20]. The colloidal crystal templating method may be used in combination with sol–gel, salt-solution, nanocrystalline and other precursors to produce the inorganic 3D macrostructures [20]. The different synthesis methods to produce 3D ordered macroporous structures have been recently reviewed by Guliants et al. [42]. The colloidal crystal templates used to prepare 3D macroporous materials include monodisperse polystyrene (PS), polymethyl methacrylate (PMMA) and silica spheres. Prior to precursor infiltration, these monodisperse spheres are ordered into close-packed arrays by sedimentation, centrifugation, vertical deposition or electrophoresis [43]. The final inorganic macroporous structure after the removal of spheres contains ordered interconnected pore structure shown in Fig. 4.

Macroporous vanadium-phosphorus-oxide (VPO) phases with remarkable compositional, structural and morphological properties have been synthesized by employing monodisperse polystyrene sphere arrays as a template [44,45]. Colloidal polystyrene spheres were ordered into closed-packed arrays by sedimentation or centrifugation. Depending on the choice of VPO sources and template removal method, various crystalline VPO phases were obtained. The macroscale-templated synthesis produced VPO phases with unprecedented high surface areas (75 m^2/g), desirable macroporous architecture, optimal bulk compositions (P/V ~ 1.1), desirable vanadium oxidation states (+4.1–4.4) and preferential exposure of the surface (1 0 0) planes of vanadyl(IV) pyrophosphate, $VO_2P_2O_7$, the proposed active and selective phase for *n*-butane oxidation to maleic anhydride.

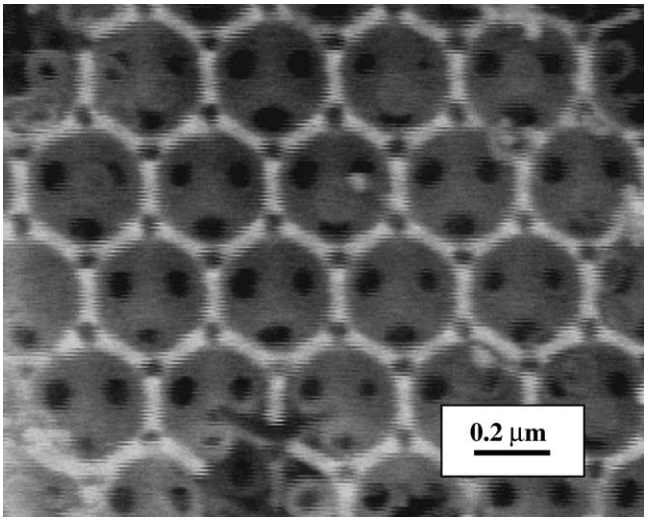

Fig. 4. SEM image of *macroporous* vanadium-phosphorus-oxide [54].

The ability to control the inorganic wall thickness, pore size, elemental and phase compositions makes the colloidal sphere array templating a versatile, attractive and flexible route for the synthesis of highly ordered macroporous phases with fine-tuned pore and framework architectures. The wall thickness of macroporous structures can be controlled by the hydrolysis/condensation rates of the inorganic precursors [46], the PS sphere packing [45] and by forming core–shell structures at the sphere surface (i.e. deposition of polyelectrolyte multilayers at the sphere surface) [47]. The pore size can be easily manipulated in the range of the sphere sizes, which are typically 100 nm to 50 μm in diameter. Even smaller spheres (20 nm) can be prepared and used to template small-pore materials [43]. Furthermore, it is possible to build macroporous structures containing a specific crystalline phase by incorporating nanoparticles of desired phases in the voids of sphere arrays [48]. Depending on the choice of the inorganic sources and template removal method, various crystalline phases can be obtained [45]. This suggests that the most critical aspects in the preparation of these macroporous structures are the ability of the precursors to infiltrate and condense between the spaces of the colloidal spheres without swelling or destroying the template as well as the ability to avoid excessive grain growth which leads to a decrease in macroporosity and structural order. Due to their high surface areas, unimodal large pores and nanocrystalline walls, these macroporous structures are highly attractive for a variety of catalytic applications.

4. Emerging applications in selective oxidation of hydrocarbons

Some early examples of catalytic mesoporous *silicates* have been reviewed by Sayari [49]. However, only few reports exist on catalytic applications of *bulk mixed*

Table 1
Emerging catalytic applications of mesoporous and macroporous bulk *mixed* metal oxides in selective oxidation reactions

Oxide system[a]	Reaction	Product	Reaction conditions	Activity/selectivity	Ref.
Meso-Fe_2O_3–**TiO_2**	Cyclohexane oxidation	Cyclohexanol, cyclohexanone, isobutyraldehyde, acetic acid	T = 343 K, P = 1 atm, time = 15–17 h	Conversion = 25.8%, selectivity to cyclohexanol and cyclohexanone = 90%	[50]
Meso-VO_x–**TiO_2**	Propene oxidation	CO + CO_2	T = 500 K, P_{O_2} = 6.6 kPa, $P_{C_3H_6}$ = 2.4 kPa	Activity (min^{-1}) CO = 0.091, CO_2 = 0.279, selectivity to CO_2 = 75%	[51]
Meso-**VPO**	*n*-Butane oxidation	Maleic anhydride	T = 673 K, 1.7% *n*-butane in air, space velocity F/V = 55 min^{-1}	*n*-Butane conversion = 10%, selectivity to maleic anhydride= 40%	[33]
Macro-**VPO**	*n*-Butane oxidation	Maleic anhydride	T = 673 K, 1.4% *n*-butane in air, space velocity F/V = 55 min^{-1}	*n*-Butane conversion = 90%, selectivity to maleic anhydride = 60%	[54]
Macro-**VPO**	Propene ammoxidation	Acetonitrile, acrylonitrile, acrolein	T = 753 K, 25% O_2, 9.8% propane, 8.6% ammonia, balance helium flow rate 10 cm^3/min	Yields: acetonitrile (15.7%), acrylonitrile (20.3%), acrolein (7.8%)	[54]

[a] Letters in bold refer to mesoporous oxides.

mesoporous metal oxides. Gedanken and coworkers [50] studied the oxidation of cyclohexane to cyclohexanol and cyclohexanone over mesoporous Fe_2O_3–TiO_2 catalyst. The mesoporous catalysts displayed ~5% higher cyclohexane conversion under the same conditions as compared to catalysts in which Fe_2O_3 was incorporated in non-porous TiO_2. Yoshitake and Tatsumi [51] incorporated V oxide into mesoporous TiO_2 and studied these novel catalysts in propene oxidation reaction. They found that the rate of propene oxidation to CO and CO_2 was ~18 times higher on mesoporous VO_x–TiO_2 catalysts as compared to conventional VO_x–TiO_2 (i.e. non-porous TiO_2 matrix). The high surface areas displayed by these mesoporous catalysts and improved dispersion of active surface sites in the mesoporous hosts were responsible for their enhanced catalytic performance. The catalytic performance of ordered mesostructured vanadium-phosphorus-oxides in selective *n*-butane oxidation was studied by Guliants et al. [33] Mesostructured VPO was evaluated in *n*-butane oxidation to maleic anhydride. Selectivities to maleic anhydride up to ~40 mol% were observed at 673K at ~10% *n*-butane conversions. A conventional organic VPO catalyst containing well-crystallized vanadyl(IV) pyrophosphate, the proposed active and selective phase for *n*-butane oxidation to maleic anhydride, displayed the selectivities to maleic anhydride of ~50 mol% under the same reaction conditions. The limited thermal stability of mesostructured VPO during *n*-butane oxidation led to the gradual loss of the structural order and poor catalytic performance. These results further suggested that the vanadyl(IV) pyrophosphate phase is required for this alkane oxidation reaction.

Only few examples of catalytic macroporous *silicates* have been reported [52,53]. Stein and coworkers [52,53] used ordered macroporous *silica* as a support for catalytically active species. For instance, the Stein group found that γ-$SiW_{10}O_{36}$ polyoxometallate clusters incorporated into the walls of macroporous silica exhibited catalytic activity for the epoxidation of cyclooctene [52]. In another study, Johnson and Stein [53] compared different pore structures (macro, meso and non-porous silica surfaces) with the activity of silica samples doped with transition metal substituted polyoxometallates (TMSP). Although the three types of catalysts showed comparable conversions in the epoxidation of cyclohexene to cyclohexene oxide, the open macroporous structure supported a greater number of TMSP clusters at its surface leading to improved cluster retention during the catalytic reaction.

Recently reported macroporous VPO represents the first example of a bulk macroporous transition *mixed* metal oxide employed in the selective oxidation of lower alkanes [54]. The catalytic performance of this VPO phase was evaluated in the partial oxidation of *n*-butane to maleic anhydride. The observed yield of maleic anhydride was >50% for macroporous VPO [54]. Under similar reaction conditions, the yield of maleic anhydride was ~40% for the conventional organic VPO catalyst. The ordered open pore structures, the high surface areas (>40 m^2/g) and the presence of nanocrystalline $(VO)_2P_2O_7$ in macroporous VPO resulted in improved catalytic performance. Table 1 summarizes the reported examples of mesoporous and macroporous mixed metal oxide catalysts for selective oxidation of hydrocarbons.

5. Concluding remarks

The meso and macroscale self-assembly approaches are particularly attractive for the design of novel bulk catalytic phases on multiple length scales that possess unique pore structures, flexible compositions and tunable surface active sites. These unique porous structures with finely tuned surface active sites are highly promising as improved catalysts for a variety of selective alkane oxidation reactions. Moreover, it is expected that these novel model catalytic systems would lead

to improved fundamental understanding of the relationships between the molecular structure and catalytic properties of a broad range of industrially relevant catalytic systems.

References

[1] F. Trifirò, Catal. Today 41 (1–3) (1998) 21.
[2] F. Cavani, F. Trifirò, Catal. Today 51 (3–4) (1999) 561.
[3] G. Centi, F. Cavani, F. Trifirò, Selective Oxidation by Heterogeneous Catalysis. Fundamental and Applied Catalysis, Kluwer Academic Publishers/Plenum Press, 2001.
[4] S. Albonetti, F. Cavani, F. Trifirò, Catal. Rev. 38 (4) (1996) 413.
[5] G. Centi, F. Trifirò, Appl. Catal. 12 (1) (1984) 1.
[6] D.J. Hucknall, Selective Oxidation of Hydrocarbons, Academic Press, London, 1974.
[7] V.V. Guliants, J.B. Benziger, S. Sundaresan, I.E. Wachs, J.-M. Jehng, J.E. Roberts, Catal. Today 28 (4) (1996) 275.
[8] F. Cavani, F. Trifirò, Appl. Catal. 88 (1992) 115.
[9] F. Cavani, F. Trifirò, ChemTech 24 (1994) 18.
[10] F. Cavani, F. Trifirò, Stud. Surf. Sci. Catal. 91 (1995) 1.
[11] G. Centi, F. Trifirò, J.R. Ebner, V.M. Franchetti, Chem. Rev. 88 (1) (1988) 55.
[12] F. Trifirò, Catal. Today 16 (1) (1993) 91.
[13] K. Ruth, R. Burch, R. Kieffer, J. Catal. 175 (1998) 27.
[14] M. Takahashi, X. Tu, T. Hirose, M. Ishii, assigned to Toagosei Co. Ltd., Japan, US Patent 5,994,580 (1999).
[15] G. Centi, S. Perathoner, F. Trifirò, Appl. Catal. A 157 (1–2) (1997) 143.
[16] J.N. Al-Saeedi, V.K. Vasudevan, V.V. Guliants, Catal. Commun. 4 (2003) 537.
[17] C.T. Kresge, M.E. Leonowicz, W.J. Roth, J.C. Vartuli, J.S. Beck, J. S. Nature 359 (1992) 710.
[18] J.S. Beck, J.C. Vartuli, W.J. Roth, M.E. Leonowicz, C.T. Kresge, K.D. Schmitt, C.T.-W. Chu, D.H. Olson, E.W. Sheppard, S.B. McCullen, J.B. Higgins, J.L. Schlenker, J. Am. Chem. Soc. 114 (1992) 10834.
[19] C.T. Kresge, M.E. Leonowicz, W.J. Roth, J.C. Vartulli J.C., Mobil Oil Corp., US Patent 5,098,684 (1992).
[20] A. Stein, R.C. Schroden, Curr. Opin. Solid State Mater. Sci. 5 (2001) 553.
[21] Q. Huo, D.I. Margolese, G.D. Stucky, Chem. Mater. 8 (1996) 1147.
[22] S.A. Bagshaw, E. Prouzet, T.J. Pinnavaia, Science 269 (1995) 1242.
[23] D. Zhao, J. Feng, Q. Huo, N. Melosh, G.H. Fredickson, B.F. Chmelka, G.D. Stucky, Science 279 (1998) 548.
[24] D.M. Antonelli, J.Y. Ying, Mesoporous Materials, Curr. Opin. Coll. Interf. Sci. 1 (1996) 523.
[25] R.M. Contractor, H.S. Horowitz, G.S. Patience, J.D. Sullivan, to E.I. DuPont de Nemours and Company, US Patent 5,895,821 (1999).
[26] T. Abe, A. Taguchi, M. Iwamoto, Chem. Mater. 7 (1995) 1429.
[27] T. Doi, T. Miyake, Chem. Commun. (1996) 1635.
[28] J.E. Haskouri, M. Roca, S. Cabrera, J. Alamo, A. Beltran-Porter, D. Beltran-Porter, M.D. Marco, P. Amoros, Chem. Mater. 11 (1999) 1446.
[29] N. Mizuno, H. Hatayama, S. Uchida, A. Taguchi, Chem. Mater. 13 (2001) 179.
[30] M.A. Carreon, V.V. Guliants, Micropor. Mesopor. Mater. 55 (2002) 297.
[31] M.A. Carreon, V.V. Guliants, Stud. Surf. Sci. Catal. 141 (2002) 301.
[32] M.A. Carreon, V.V. Guliants, Catal. Today 78 (2003) 303.
[33] M.A. Carreon, V.V. Guliants, F. Pierelli, F. Cavani, Catal. Lett. 92 (2004) 11.
[34] B. Lee, T. Yamashita, D. Lu, J.N. Kondo, K. Domen, Chem. Mater. 14 (2002) 867.
[35] X. He, A.Y.H. Lo, M. Trudeau, R.W. Schurko, D. Antonelli, Inorg. Chem. 42 (2003) 335.
[36] Z.-S. Chao, E. Ruckenstein, Langmuir 18 (2002) 734.
[37] Z.-S. Chao, E. Ruckenstein, Langmuir 18 (2002) 8535.
[38] R.J. Hunter, Zeta Potential in Colloid Science: Principles and Applications, Academic Press, London, 1981.
[39] T.J. Gray, et al. The Defect Solid State, Interscience, New York, 1957, p. 96.
[40] A.T. Bell, Science 299 (2003) 1688.
[41] R.C. Weast, M.J. Astle, W.H. Beyer (Eds.), CRC Handbook of Chemistry and Physics: A Ready-reference Book of Chemical and Physical Data, 67th ed. CRC Press, Boca Raton, FL, 1986.
[42] V.V. Guliants, M.A. Carreon, Y.S. Lin, J. Membr. Sci. 235 (1–2) (2004) 53.
[43] Y. Xia, B. Gates, Y. Yin, Y. Lu, Adv. Mater. 12 (2000) 693.
[44] M.A. Carreon, V.V. Guliants, Chem. Commun. (2001) 1438.
[45] M.A. Carreon, V.V. Guliants, Chem. Mater. 14 (6) (2002) 2670.
[46] B.T. Holland, C.F. Blanford, T. Do, A. Stein, Chem. Mater. 11 (1999) 795.
[47] D. Wang, R.A. Caruso, F. Caruso, Chem. Mater. 13 (2001) 364.
[48] G. Subramanian, V.N. Manoharan, J.D. Thorne, D.J. Pine, Adv. Mater. 11 (15) (1999) 1261.
[49] A. Sayari, Chem. Mater. 8 (1996) 1840.
[50] N. Perkas, Y. Wang, Y. Koltypin, A. Gedanken, S. Chandrasekaran, Chem. Commun. 11 (2001) 988.
[51] H. Yoshitake, T. Tatsumi, Chem. Mater. 15 (2003) 1695.
[52] R.C. Schroden, C.F. Blanford, B.J. Melde, B.J.S. Johnson, A. Stein, Chem. Mater. 13 (2001) 1074.
[53] B.J.S. Johnson, A. Stein, Inorg. Chem. 40 (2001) 801.
[54] M.A. Carreon, Ph.D. Thesis, University of Cincinnati, 2003.